



## FULL LENGTH ARTICLE

# Melatonin antagonizes ovarian aging via YTHDF2-MAPK-NF- $\kappa$ B pathway

Ruigong Zhu<sup>a,1</sup>, Xian Ji<sup>a,1</sup>, Xuan Wu<sup>a,1</sup>, Jiajing Chen<sup>a</sup>,  
 Xuesong Li<sup>a</sup>, Hong Jiang<sup>a</sup>, Haiping Fu<sup>a</sup>, Hui Wang<sup>a</sup>, Zhe Lin<sup>a</sup>,  
 Xin Tang<sup>a</sup>, Shixiu Sun<sup>a</sup>, Qingguo Li<sup>b,\*\*\*</sup>, Bingjian Wang<sup>d,\*\*</sup>,  
 Hongshan Chen<sup>a,b,c,d,\*</sup>

<sup>a</sup> Key Laboratory of Cardiovascular & Cerebrovascular Medicine, School of Pharmacy, Nanjing Medical University, Nanjing, Jiangsu 211166, PR China

<sup>b</sup> Department of Cardiothoracic Surgery, The Second Affiliated Hospital of Nanjing Medical University, Nanjing, Jiangsu 210003, PR China

<sup>c</sup> Key Laboratory of Targeted Intervention of Cardiovascular Disease, Collaborative Innovation Center for Cardiovascular Disease Translational Medicine, Nanjing Medical University, Nanjing, Jiangsu 211166, PR China

<sup>d</sup> Department of Cardiology, Huai'an First People's Hospital Affiliated with Nanjing Medical University, Huai'an, Jiangsu 223399, PR China

Received 30 May 2020; received in revised form 29 July 2020; accepted 16 August 2020  
 Available online 21 August 2020

## KEYWORDS

Gene expression;  
 Inflammation;  
 Melatonin;  
 Senescence;  
 YTHDF2

**Abstract** Cellular senescence is closely associated with age-related diseases. Ovarian aging, a special type of organ senescence, is the pathophysiological foundation of the diseases of the reproductive system. It is characterized by the loss of integrity of the surface epithelium and a gradual decrease in the number of human ovarian surface epithelial cells (HOSEpiCs). To contribute to the research on delaying ovarian aging, we aimed to investigate the novel epigenetic mechanism of melatonin in protecting HOSEpiCs. We discovered that melatonin has antagonistic effects against the oncogene-induced senescence (OIS) of HOSEpiCs. Mechanistically, the oncogene Ras decreased the expression of YTHDF2, which is the reader of RNA-m<sup>6</sup>A, by stimulating the generation of reactive oxygen species (ROS). Moreover, we found that the suppression of YTHDF2 increased the expression of MAP2K4 and MAP4K4 by enhancing the stability of the transcription of their mRNAs, thereby upregulating the expression of the senescence-associated secretory phenotype (SASP) through the activation of the MAP2K4

\* Corresponding author. Key Laboratory of Cardiovascular & Cerebrovascular Medicine, School of Pharmacy, Nanjing Medical University, Nanjing, Jiangsu 211166, PR China.

\*\* Corresponding author.

\*\*\* Corresponding author.

E-mail addresses: [lqg0235062@163.com](mailto:lqg0235062@163.com) (Q. Li), [wofcardio96@126.com](mailto:wofcardio96@126.com) (B. Wang), [hongshan.chen@njmu.edu.cn](mailto:hongshan.chen@njmu.edu.cn) (H. Chen).

Peer review under responsibility of Chongqing Medical University.

<sup>1</sup> Ruigong Zhu, Xian Ji and Xuan Wu contributed equally to this work.

<https://doi.org/10.1016/j.gendis.2020.08.005>

2352-3042/Copyright © 2020, Chongqing Medical University. Production and hosting by Elsevier B.V. This is an open access article under the CC BY-NC-ND license (<http://creativecommons.org/licenses/by-nc-nd/4.0/>).

and MAP4K4-dependent nuclear factor- $\kappa$ B (NF- $\kappa$ B) signaling pathways. We further determined that melatonin has antagonistic effects against the OIS of HOSEpiCs by inhibiting the ROS-YTHDF2-MAPK-NF- $\kappa$ B pathway. These findings provide key insights into the potential avenues for preventing and treating ovarian aging.

Copyright © 2020, Chongqing Medical University. Production and hosting by Elsevier B.V. This is an open access article under the CC BY-NC-ND license (<http://creativecommons.org/licenses/by-nc-nd/4.0/>).

## Introduction

Aging is gradually becoming a serious threat to human health worldwide.<sup>1</sup> Cellular senescence, which is a permanent hyporeplicative state induced by stress, is emerging as a fundamental aging mechanism.<sup>2</sup> Senescent cells are usually characterized by the expression of anti-proliferative molecules (e.g., p16INK4a cell cycle inhibitor), dysfunctional telomeres, and senescence-associated secretory phenotype (SASP).<sup>3</sup> Numerous studies have confirmed that the steady accumulation of senescent cells contributes to many age-related diseases, including cancer, atherosclerosis, and neurogenesis.<sup>1</sup> Therefore, therapeutic strategies that target the underlying mechanism of senescence may effectively attenuate the progression of age-related diseases.

Ovarian aging is a long-term and complex process that leads to the decreased quantity and quality of oocytes, a marked decline in the pool of follicles, and female infertility.<sup>4,5</sup> Natural aging and the treatment of ovarian cancer with various chemotherapeutic drugs accelerate ovarian aging; several therapeutic strategies, such as androgen supplementation, short-term rapamycin treatment, and moxibustion, are available but remain uncomprehensive.<sup>6–8</sup> Therefore, it is necessary to further understand the mechanisms of senescence and discover novel drug targets as well as therapies.

Inflammation is one of the major contributors to senescence.<sup>9,10</sup> The SASP, which is known for altering the secretory activities of senescent cells, includes pro-inflammatory cytokines, chemokines, growth factors, and proteases.<sup>11,12</sup> RNA modification, which is considered a mode of post-transcriptional gene regulation, has been reported in several papers.<sup>13,14</sup> N6-methyladenosine (m<sup>6</sup>A) is an RNA modification that is closely related to inflammatory response.<sup>15</sup> m<sup>6</sup>A, a common internal decoration on eukaryotic mRNAs, plays a pivotal role in regulating various biological processes.<sup>13,16</sup> It exerts a regulatory effect by interacting with m<sup>6</sup>A readers<sup>17</sup> such as YTH domain-containing proteins (YTHDF1, YTHDF2, YTHDF3, YTHDC1, and YTHDC2), eukaryotic translation initiation factor 3, heterogeneous nuclear ribonucleoprotein (hnRNP) C, hnRNP G, and hnRNP A2B1.<sup>18</sup> Recent studies have reported that m<sup>6</sup>A is involved in inflammation and senescence and, especially, in ovarian aging.<sup>15,19,20</sup> Thus, we sought to elucidate the molecular mechanism of m<sup>6</sup>A in ovarian aging and explore whether m<sup>6</sup>A can serve as a potential target for preventing or treating ovarian aging.

Melatonin, produced and released from the pineal gland, is known as a prime regulator of human chronobiological and endocrine physiology.<sup>21</sup> The melatonin levels in pineal and blood provide information on light or darkness via peaking during darkness and plunging during the day.<sup>22</sup>

Besides pineal gland, melatonin could be synthesized in the mitochondria of all kinds of cells.<sup>23,24</sup> Melatonin possesses potent anti-oxidant, anti-inflammatory, anti-aging, onco-static, and endocrine-modulating effects.<sup>25</sup> It was also reported that melatonin delays ovarian aging by multiple mechanisms such as anti-oxidant action and stimulating SIRT expression<sup>4</sup>; however, numerous pharmacological mechanisms remain to be explored such that better treatment of this kind of disease is facilitated. Moreover, a recent study<sup>26</sup> reported that melatonin is involved in the regulation of m<sup>6</sup>A; this prompted the further exploration of whether melatonin participates in anti-aging, inflammation, and SASP through a mechanism that regulates m<sup>6</sup>A, such that a therapeutic effect is achieved.

This study aimed to investigate a novel mechanism through which melatonin can diminish ovarian aging. We screened the primary factors involved in aberrant m<sup>6</sup>A modification and identified that the oncogene Ras could induce an abnormally decreased expression of YTHDF2 in human ovarian surface epithelial cells (HOSEpiCs) with SASP. Furthermore, we found that melatonin delayed oncogene-induced senescence (OIS) in HOSEpiCs by upregulating the expression of YTHDF2, thereby inhibiting the expression of SASP via the inactivation of the MAPK-NF- $\kappa$ B signaling pathway. The elucidation of the mechanisms underlying the anti-senescence effects of melatonin would have significant implications for developing novel therapies for ovarian aging.

## Materials and methods

### Cell culture and treatment

Human ovarian surface epithelial cells were obtained from American Type Culture Collection (ATCC) and were cultured at 37 °C in 5% carbon dioxide and RPMI-1640 medium supplemented with 10% fetal bovine serum (FBS), 100 units/ml penicillin and 100 µg/mL streptomycin. Senescence of human ovarian surface epithelial cells was induced using OIS as previously described.<sup>27</sup> OIS was induced by retroviral-mediated ectopic expression of H-RasV12 or an empty vector (as a control). Cells were treated with 1 µM melatonin (Sigma, M5250, Germany) or 10 mM N-acetyl-L-cysteine (NAC) (Sigma, A7250, Germany) for indicated time. Cells were transfected with small interfering RNA (siRNA) or negative control siRNA (Shanghai GenePharma, China) using Lipofectamine 3000 Reagent (Invitrogen, USA) following the manufacturer's protocols. The most efficient one was selected for the following studies. A scrambled duplex RNA oligo was used as the negative control (NC). HOSEpiCs expressing YTHDF2 were generated by plasmids transduction with the pQCXIP expression system (Clontech Laboratories, USA) according to the manufacturers' instructions.

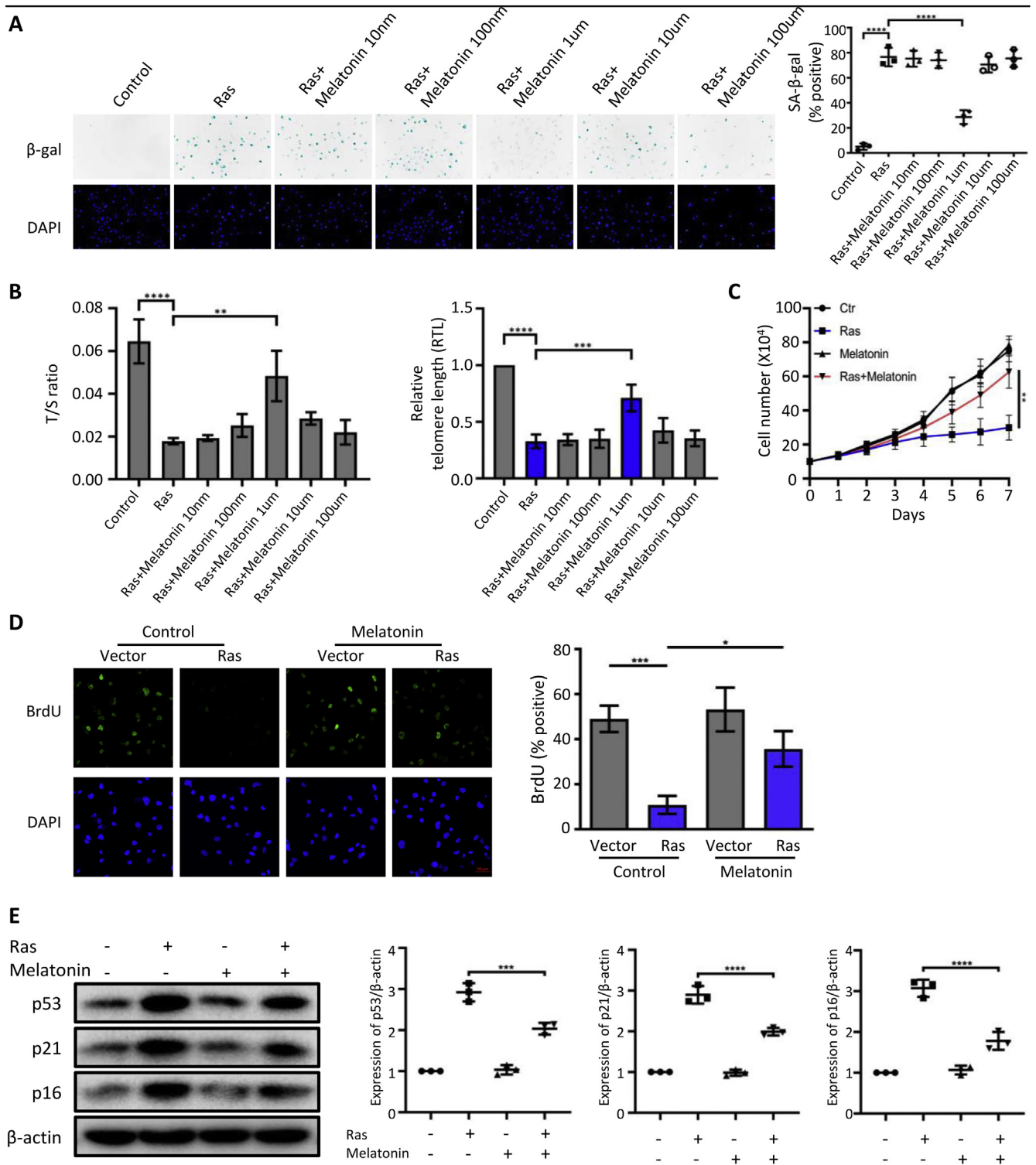
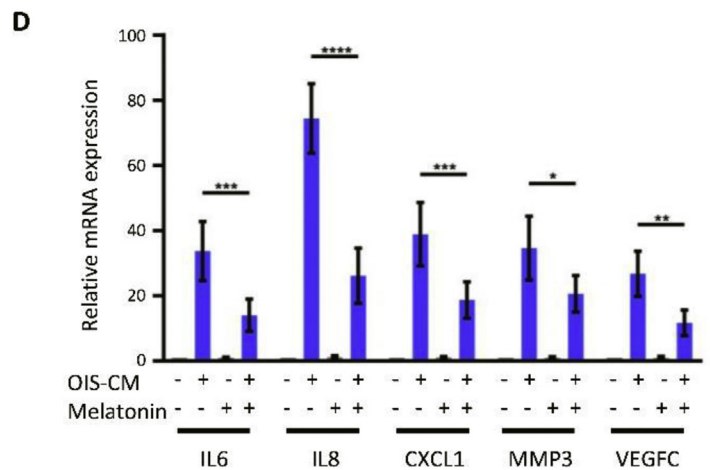
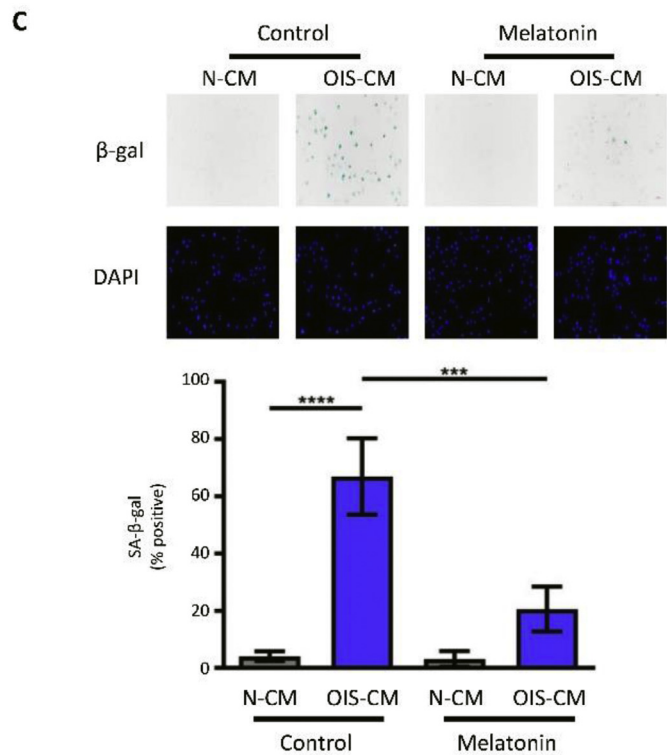
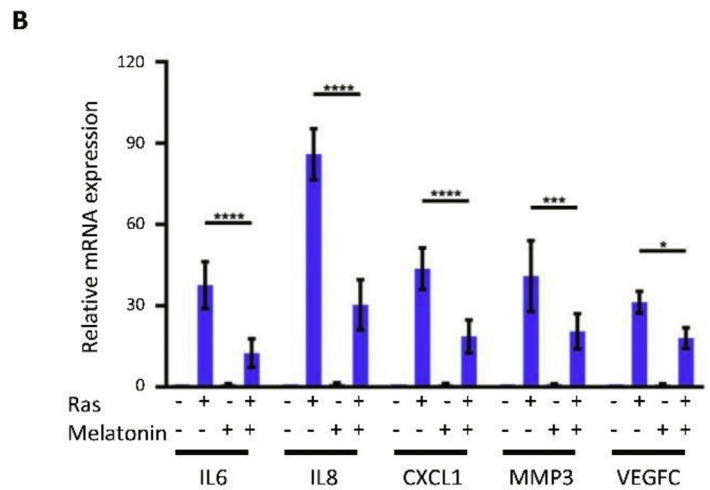
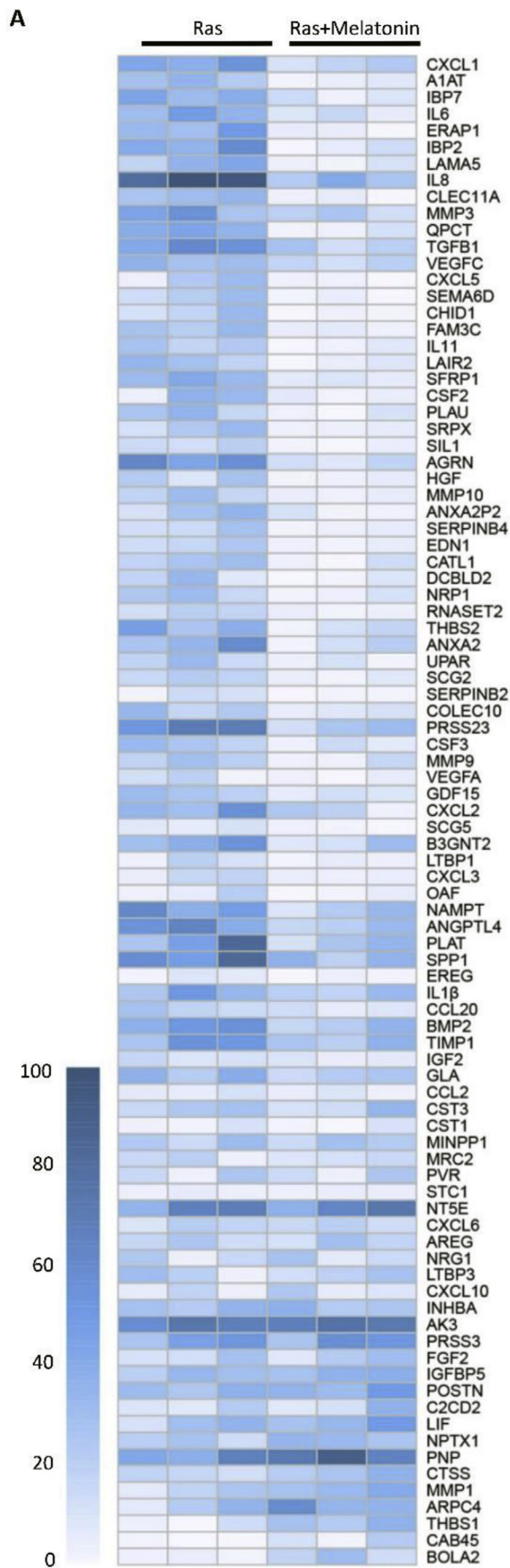


**Figure 1** Antagonistic effect of melatonin against OIS-induced senescence of human ovarian surface epithelial cells. (A) HOSEpiCs were subjected to the retrovirus-mediated gene transfer of H-RasV12 or of an empty vector as a control and treated with melatonin at 10 nM, 100 nM, 1  $\mu$ M, 10  $\mu$ M, and 100  $\mu$ M concentrations. Representative senescence-associated  $\beta$ -galactosidase staining (SA- $\beta$ -gal) and 4',6-diamidino-2-phenylindole (DAPI) staining images of HOSEpiCs and percent SA- $\beta$ -gal-positive cells; scale bar, 50  $\mu$ m. (B) Ratio of telomere to single copy gene expression (T/S) of the HOSEpiCs and the relative telomere lengths computed from T/S. (C) Growth curves of HOSEpiCs treated as described in (A). Number of cells from each group counted at the indicated time points. (D) Representative immunofluorescence images of BrdU-labelled and DAPI-counterstained HOSEpiCs transfected with an H-RasV12 or an empty control vector, where indicated, treated with (+) or without (-) 1  $\mu$ M melatonin for 8 days. Histogram of BrdU-positive cells treated as described above. (E) The senescent markers p53, p21, and p16 were analyzed by Western blotting. The results are presented in the scatter plot.  $\beta$ -actin was used as the loading control. Statistical values are presented as the mean  $\pm$  standard error of the mean of three independent experiments. A  $P < 0.05$  was considered statistically significant using one-way analysis of variance. \*,  $P < 0.05$ .



### Senescence-associated $\beta$ -galactosidase (SA- $\beta$ -Gal staining) activity

Following a previous protocol, SA- $\beta$ -Gal staining was performed with slight modification.<sup>28</sup> The cells were fixed and incubated overnight at 37 °C using a Senescence  $\beta$ -Galactosidase Staining Kit (Beyotime Biotechnology, China) according to the manufacturer's instructions. Stained and unstained cells were imaged with a fluorescence microscope (Nikon, Japan).

### Western blotting

Cells were harvested in RIPA (Beyotime, China) buffer including protease inhibitor phenylmethylsulfonyl fluoride (PMSF) (Beyotime, China) on ice. Proteins from each sample were quantified using a BCA Protein Assay kit (Beyotime, China). After equal amounts of protein samples were run on sodium dodecyl sulfate–polyacrylamide gel electrophoresis (SDS-PAGE) and transferred onto polyvinylidene difluoride membranes (Millipore, Billerica, MA, USA), the membranes were blocked in 5% skimmed milk for 1 h at room temperature. Then, some specific primary antibodies were used to incubate the membranes at 4 °C overnight. Various selected proteins were detected using the appropriate secondary antibody for 1 h at room temperature. Finally, the immunoreactive bands were visualized by Pierce ECL Western Blotting Substrate. The antibodies used for blotting are shown in Table S1.

### Real-time quantitative polymerase chain reaction (qRT-PCR)

Total RNA was extracted using Trizol reagent (Invitrogen, USA) according to the manufacturer's instructions followed by reverse transcription with HiScript-II-Q RT SuperMix for qPCR (Vazyme, Nanjing, China). qRT-PCR was performed using an ABI 7500 Real-Time PCR System (Applied Biosystems, Foster City, CA, USA). Actin was used for the normalization of gene expression values. The comparative Ct method was used to analyze the raw data (Ct values). All primers were synthesized by a commercial vendor (Nanjing Genesay, China) and the sequences are listed in Table S2.

### Immunofluorescence

Cells cultured in glass-bottomed culture dishes were fixed in 4% paraformaldehyde for 20 min and then permeabilized with 0.5% Triton X-100 for 20 min. Then, the cells were blocked with 3% BSA for 1 h, followed by incubation with

the specific primary antibody at 4 °C overnight. After washing with PBS, cells were incubated with the secondary antibody for 1 h at 37 °C and nuclei were subsequently counterstained with DAPI. Finally, the images of the labeled cells were acquired using a confocal laser scanning microscope (LSM800; Zeiss, Oberkochen, Germany).

### Quantitative real-time PCR for analysis of telomere lengths

The experiments were performed as previously described with slight modification.<sup>29</sup> The sample DNA was used as templates in the SYBR-green real-time PCR with specific telomere (T) and 36B4 (single copy gene, S) primers (Table S3). For each template DNA, a triplicate real-time reaction was run. Master mixes of PCR reagents with T and S primers were prepared in separate tubes. After performing the quantitative PCR, the ratio of T:S values was used to compute the relative telomere length (RTL).

### Reactive oxygen species measurement

The intracellular ROS levels of HOSEpiCs were measured using a ROS detection kit (Beyotime, China). The cells were incubated with 2,7-dichlorofluorescein diacetate (DCFH-DA) at 37 °C for 20 min. The cells were washed with serum-free culture twice to eliminate the unlabeled DCFH-DA. Finally, the images of the labeled cells were acquired using a fluorescence microscope (Nikon, Japan).

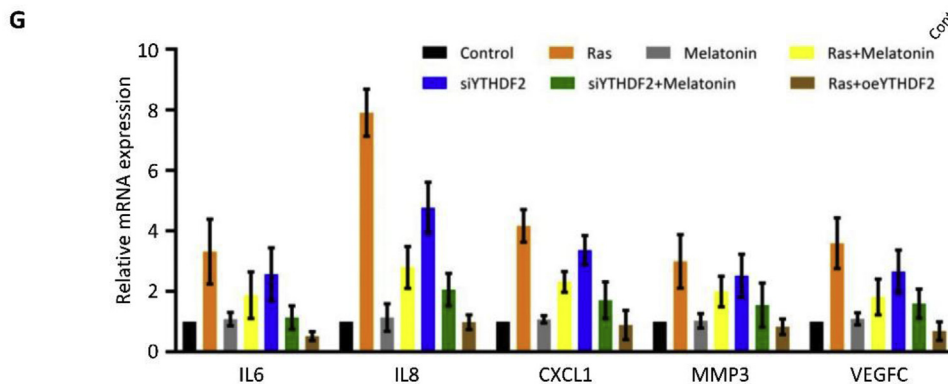
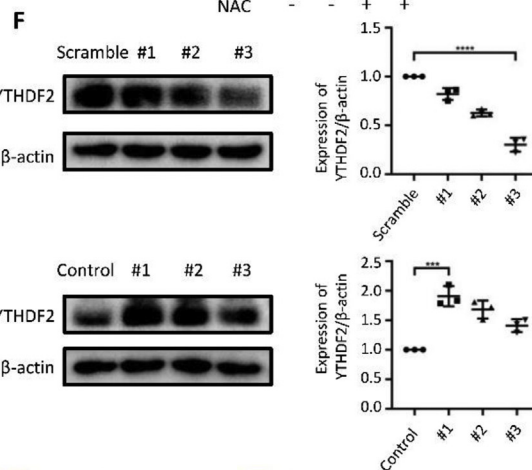
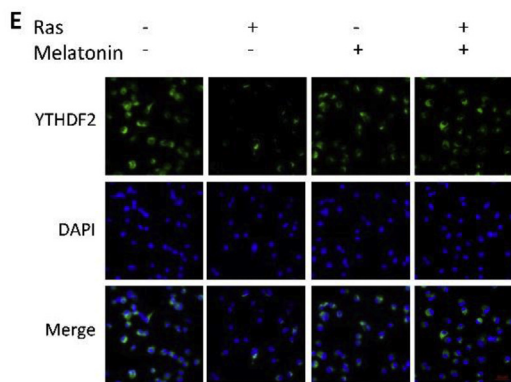
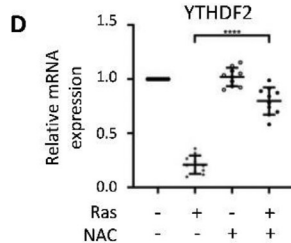
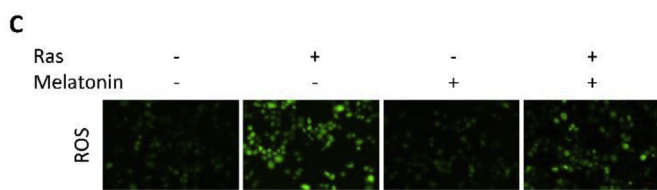
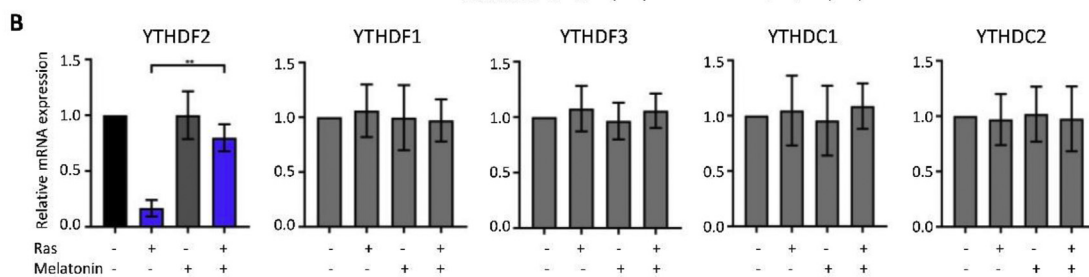
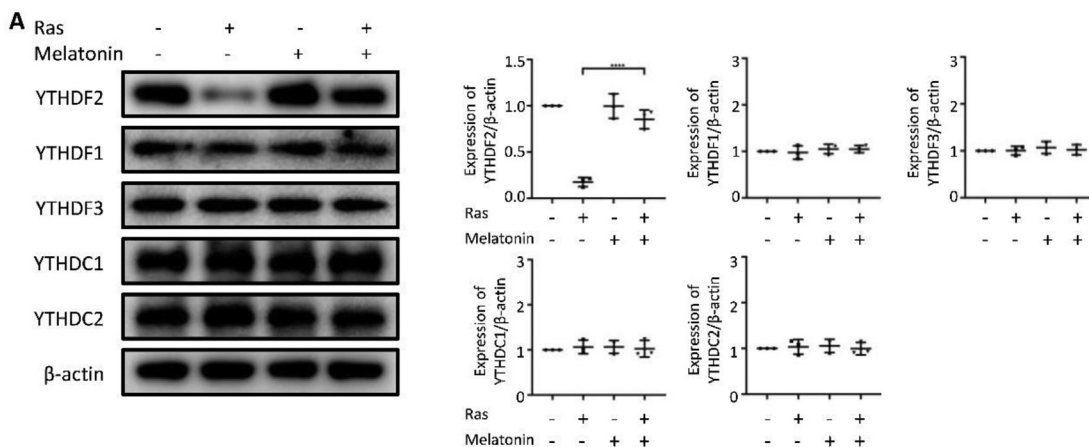
### mRNA stability assay

The experiments were performed as previously described with slight modification.<sup>30</sup> To examine the effects of YTHDF2 expression on the stability of the mRNAs of interest, actinomycin D (5  $\mu$ g/mL, Abcam, ab141058) was added to inhibit transcription after 24 h transfection. Total RNA was harvested at specific time points of 0 h, 2 h, and 4 h, then RT-PCR detected mRNA levels.

### Poly(A) tail analysis

Poly(A) tail (PAT) assay was performed as previously described with some modifications.<sup>31</sup> Briefly, total RNA was extracted using Trizol reagent (Invitrogen, USA) according to the manufacturer's instructions. R1 (5-GCGAGCTCCGCGCCGCGT12-3) was anchored to Oligo (dT) by T4 DNA ligase. Reverse transcription was performed with Oligo (dT) anchored R1. The products were used in a PCR reaction with gene-specific primers (Table S4) and the

**Figure 2** Melatonin suppresses oncogene-induced SASP. (A) qPCR array analysis was used to assess the expression of SASP genes in HOSEpiCs subjected to retrovirus-mediated H-RasV12 expression with or without melatonin treatment for 8 days. The heatmap was generated according to RT-qPCR values that are arrayed from white (low value) to blue (high value). (B) The expression of SASP genes in HOSEpiCs that were transfected with a vector containing H-RasV12 or an empty control vector and treated with or without melatonin was determined through sequencing by RT-qPCR. (C, D) HOSEpiCs cultured with conditioned medium from either H-RasV12-mediated senescent HOSEpiCs (OIS-CM) or HOSEpiCs treated with the empty control vector (N-CM) and with or without melatonin for 8 days. (C) Representative SA- $\beta$ -gal staining images and corresponding statistical data are shown. (D) The expression of SASP genes was measured using RT-qPCR. Statistical values are presented as the mean  $\pm$  standard error of the mean of three independent experiments. A  $P < 0.05$  was considered statistically significant using one-way analysis of variance. \*,  $P < 0.05$ .



dT anchor primer R1. The polyadenylation states of the PCR products were analyzed on a 1.5% agarose gel, and images were captured during exposure to ultraviolet light. Experiments were repeated multiple times to confirm reproducibility.

### Methylated RNA immunoprecipitation (MeRIP)-qPCR assay

The methylated RNA immunoprecipitation (MeRIP) assay was performed using a Magna MeRIP™ m<sup>6</sup>A kit (#17–10,499, Merck Millipore, MA, USA) as previously described.<sup>32</sup> Briefly, total RNA was isolated from HOSEpiCs by using Trizol. Total RNA (100 μg) was incubated (4 °C with mixing, overnight) with 2 μg of anti-m<sup>6</sup>A antibodies or anti-IgG and 20 μL of Dynabeads Protein G (4 °C with mixing, 6 h). After immunoprecipitation (IP), RNA was eluted from the beads. Enriched m<sup>6</sup>A modified mRNA was then detected through qPCR as described above.

### RNA immunoprecipitation (RIP)-qPCR

To examine m<sup>6</sup>A modification or RNA-binding proteins on individual genes, the Magna RIP™ Quad RNA-Binding Protein Immunoprecipitation Kit (17–704, Millipore, Billerica, MA, USA) was used according to the manufacturer's instructions. Briefly, 200 mg of total RNA was enriched with antibody- or rabbit IgG-conjugated Protein A/G Magnetic Beads in 500 mL of 1× IP buffer supplemented with RNase inhibitors at 4 °C overnight. RNA of interest was immunoprecipitated with the beads. One-tenth of each fragmented RNA sample was saved as the input control and further analyzed by qPCR.

### Chromatin immunoprecipitation (ChIP)

ChIP was performed according to the previously described.<sup>33</sup> Briefly, the cells were firstly seeded in 15-cm dishes. After different treatments, they were cross-linked in 1% formaldehyde for 10 min and then quenched in 0.125 M glycine for 5 min. The cells were collected and sonicated to generate chromatin fragments. After centrifugation, 20 μL supernatant was collected as input for quantitation and the left supernatant was diluted and precleared in protein A–agarose beads at 4 °C for 3 h. Subsequently, the supernatant was incubated with primary antibodies at 4 °C with rotation overnight followed by incubating with protein A–agarose beads at 4 °C for 2 h.

After digested in txn stop buffer (0.4 mg/mL glycogen and 0.45 mg/mL proteinase K) at 37 °C for 1 h, DNA was isolated in phenol/chloroform/isoamyl alcohol (25:24:1) and precipitated in ethanol. Finally, the enrichment of immunoprecipitated material relative to input with gene-specific primers to the specified regions was determined by qRT-PCR. The antibodies and primers used for ChIP are listed in Tables S1 and S6, respectively.

### Statistical analysis

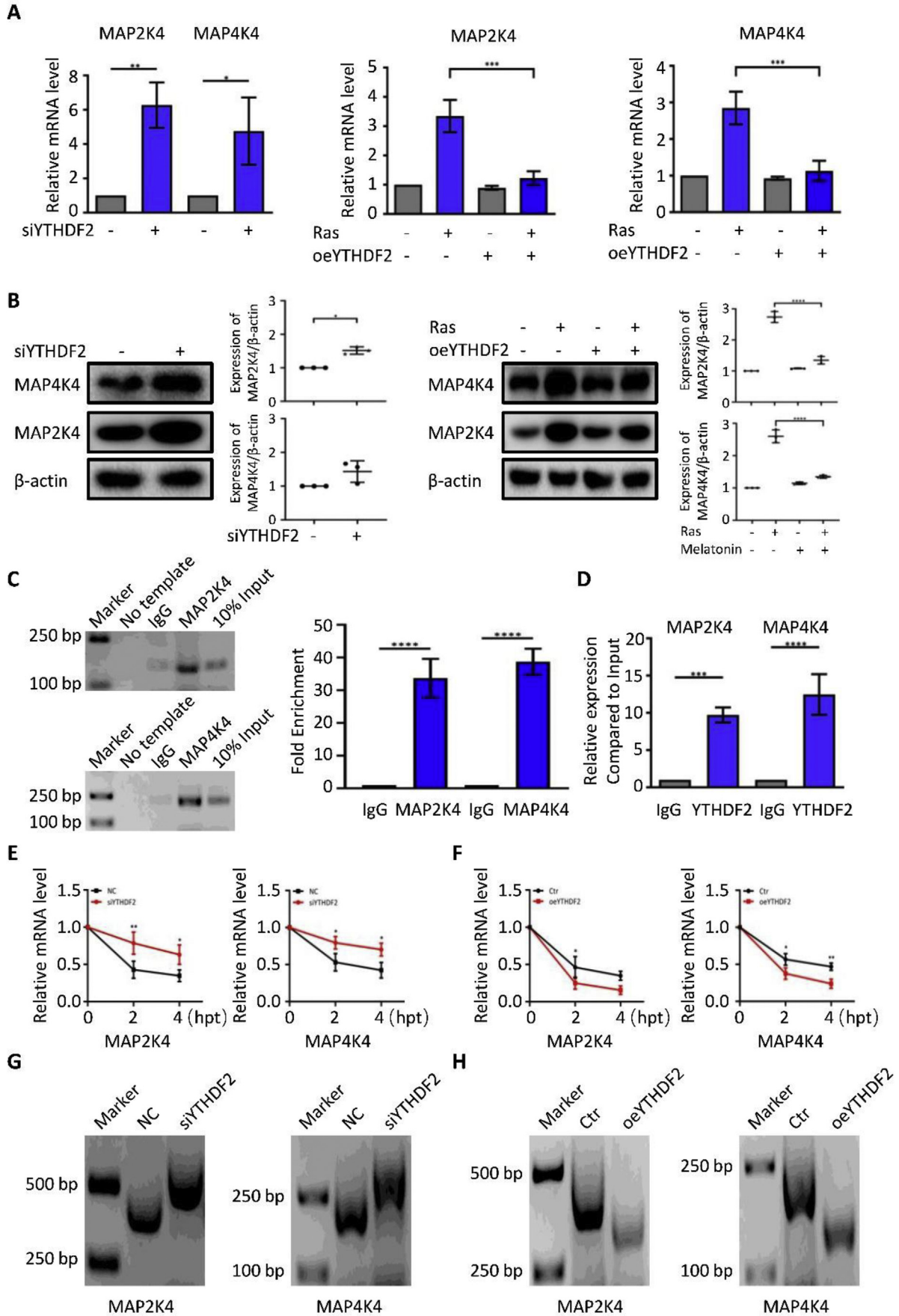
All data are presented as the median or mean ± standard error of the mean (SEM) or standard deviation (SD) of at least three independent experiments. The comparisons between experimental groups were analyzed by the Student's *t*-test and the multiple comparisons were assessed by ANOVA (analysis of variance) followed by the Sidak post-test. Data were analyzed using the Prism software v6 (GraphPad Software Inc.); *P*-values < 0.05 were considered statistically significant (\**P* < 0.05; \*\**P* < 0.01; \*\*\**P* < 0.001; \*\*\*\**P* < 0.0001).

## Results

### Antagonistic effect of melatonin against OIS in human ovarian surface epithelial cells

To investigate the role of melatonin in OIS, human ovarian surface epithelial cells (HOSEpiCs) were transfected with a vector containing H-RasV12 or an empty vector as a control. Subsequently, they were treated with melatonin at a 10 nM, 100 nM, 1 μM, 10 μM, or 100 μM concentration. The number of cells positive for SA-β-galactosidase (SA-β-gal) staining increased in response to Ras. Notably, the Ras-induced senescence of HOSEpiCs (Fig. 1A) was significantly attenuated in cells treated with 1 μM melatonin. Telomere length can be used as a predictor of the self-renewal potential of HOSEpiCs. We found that the telomeres in the Ras-treated group were shortened; the shortening of the telomeres was reversed by treatment with 1 μM melatonin (Fig. 1B). Moreover, we performed cell counting and found that the Ras-induced growth arrest of HOSEpiCs (Fig. 1C) was blocked by treatment with 1 μM melatonin for 8 days. Furthermore, using BrdU incorporation assay, we found that melatonin significantly blocked Ras-induced cell cycle arrest (0.11% in Ras-treated group vs. 0.36% in Ras and melatonin-treated group, *P* < 0.05) (Fig. 1D). Consistent with the above observations, the expression levels of the

**Figure 3** Melatonin attenuates SASP by upregulating YTHDF2. HOSEpiCs were transfected with a vector containing H-RasV12 or an empty control vector and treated with or without 1 μM melatonin. (A) Western blotting revealed the expression levels of m<sup>6</sup>A reader proteins in cells. (B) Relative mRNA levels of m<sup>6</sup>A readers were determined using RT-qPCR. (C) Representative fluorescent images of ROS in HOSEpiCs. (D) Relative mRNA levels of YTHDF2 from HOSEpiCs subjected to retrovirus-mediated expression of H-RasV12 (+) for OIS or empty vector (–) as a control and, where indicated, treated with 10 mM of the antioxidant NAC (+) or DMSO (–) for 8 days. Statistical values are presented as derived from ten independent experiments. (E) Immunofluorescence images of YTHDF2 measured by confocal microscopy. (F) The interference efficiency of YTHDF2 and the effect of YTHDF2 overexpression shown by Western blotting. HOSEpiCs were transfected with scramble as a control. (G) The expression of typical SASP genes in H-RasV12-transfected senescent HOSEpiCs transfected with either siYTHDF2 or oeYTHDF2 in the presence or absence of melatonin. Statistical values are presented as the mean ± standard error of the mean of three independent experiments. A *P* < 0.05 was considered statistically significant using one-way analysis of variance. \*, *P* < 0.05.





senescent markers p53, p21, and p16, which were upregulated by Ras, were markedly reduced by treatment with melatonin (Fig. 1E). Altogether, these observations indicated that melatonin has an antagonistic effect against the OIS-induced senescence of HOSEpiCs.

### Melatonin suppresses SASP

To evaluate the effect of melatonin on SASP, the secretome of oncogene-induced senescent HOSEpiCs was systematically analyzed using a q-PCR array. The genes of the secreted proteins in untreated and melatonin-treated HOSEpiCs were probed using RT-qPCR and defined as "OIS-induced SASP genes" as previously reported.<sup>28,34</sup> The heatmap showed that melatonin decreased the expression of the majority of OIS-induced SASP genes (Fig. 2A), which suggests that melatonin suppressed SASP. The suppressive effect of melatonin on SASP was confirmed through RT-qPCR; as H-RasV12-transfected cells were treated with melatonin, the expression of SASP-associated, functionally important factors, such as CXCL1, IL6, IL8, MMP3, and VEGFC, markedly decreased (Fig. 2B). In a study, SASP has been reported to induce paracrine senescence by secreting inflammatory cytokines.<sup>35</sup> Further experiments were performed to test whether the SASP reinforces senescence and whether the reinforced SASP expression can also be abolished by melatonin. As shown in Fig. 2C, melatonin significantly reduced the SA- $\beta$ -gal activity in HOSEpiCs that were cultured in OIS-conditioned medium (OIS-CM) with H-RasV12-transfected senescent HOSEpiCs. The elevated expression of typical SASP genes in OIS-CM-induced senescent cells was notably decreased by treatment with melatonin (Fig. 2D). In general, the results demonstrated that melatonin is crucial for suppressing the expression of oncogene-induced SASP genes and can efficiently inhibit the paracrine action of SASP.

### Melatonin attenuates SASP by upregulating YTHDF2

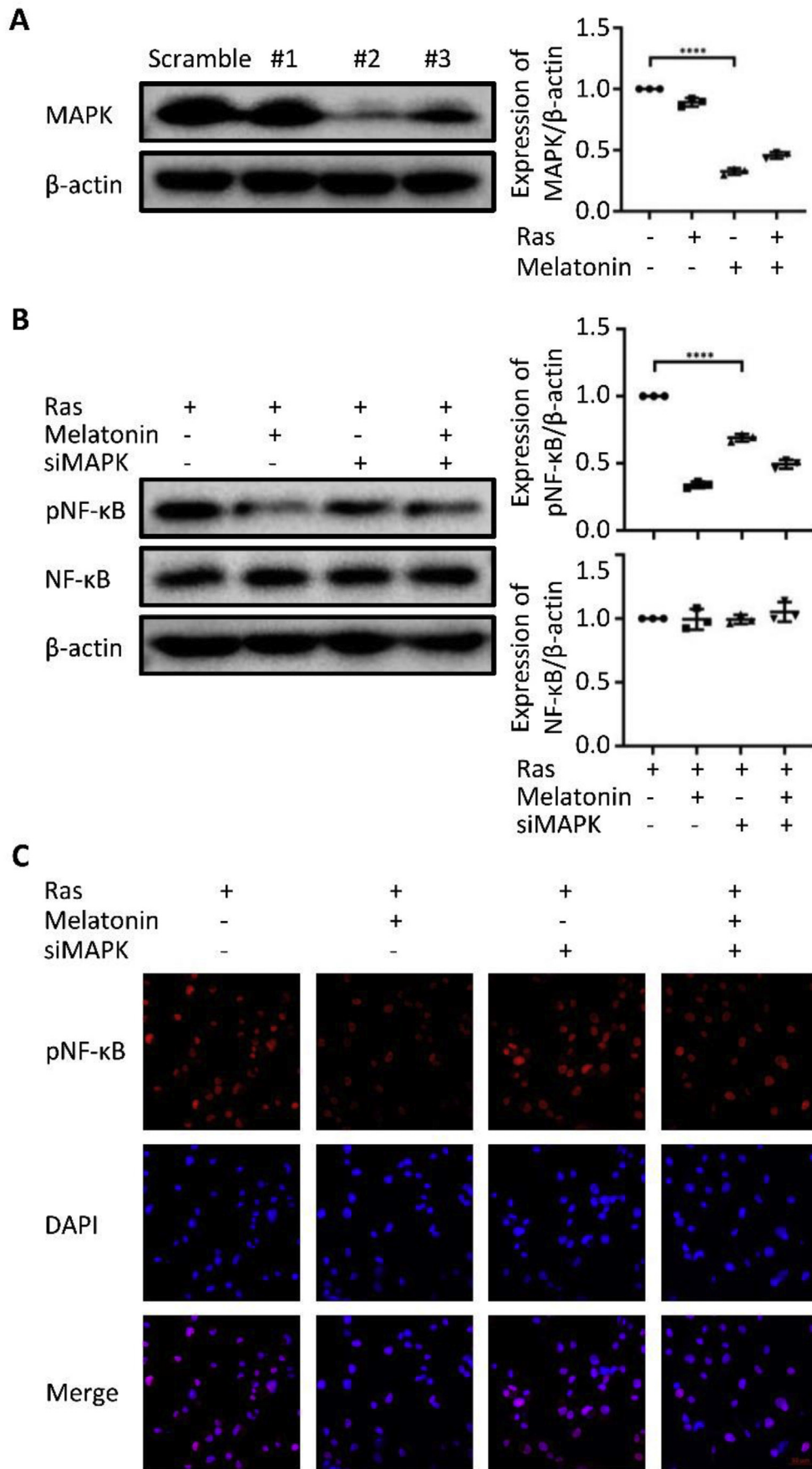
To explore the function of the m<sup>6</sup>A-binding proteins of the YTH domain family in the SASP, we first examined the expression levels of YTHDF1, YTHDF2, YTHDF3, YTHDC1, and YTHDC2 in HOSEpiCs before and after treatment with melatonin. Western blotting results showed that YTHDF2 was markedly downregulated during OIS and abrogated by melatonin (Fig. 3A); this was further confirmed using RT-qPCR (Fig. 3B) and immunofluorescence analysis (Fig. 3E). Fluorescence analysis showed that the ROS levels in Ras-

treated HOSEpiCs were increased with reference to those in the control groups; this Ras-induced ROS accumulation in HOSEpiCs was significantly attenuated by treatment with melatonin (Fig. 3C). Moreover, the use of the antioxidant N-acetyl-L-cysteine (NAC) on cells that were undergoing H-RasV12-mediated senescence significantly augmented the expression of YTHDF2; this demonstrated that an oxidative stress pathway that is transduced by elevated ROS levels exists to negatively regulate YTHDF2 expression (Fig. 3D). To further confirm the relationship between YTHDF2 and SASP, we examined the expression of the SASP-associated inflammatory factors IL6, IL8, CXCL1, MMP3, and VEGFC via the overexpression (OE) and knockdown, respectively, of YTHDF2 (Fig. 3F). The expression levels of IL6, IL8, CXCL1, MMP3, and VEGFC increased after YTHDF2 knockdown and subsequently decreased after YTHDF2 overexpression (OE), which was reversed by melatonin (Fig. 3G). Altogether, these data indicate that melatonin attenuates SASP by upregulating YTHDF2.

### Melatonin regulates the stability of MAP2K4 and MAP4K4 mRNAs in a YTHDF2-dependent manner

Previous studies have suggested that melatonin regulates senescence according to the expression of YTHDF2. Recent studies have reported that MAP2K4 and MAP4K4 act as the target genes of YTHDF2. We performed a qPCR analysis of MAP2K4 and MAP4K4 using YTHDF2 siRNA (siYTHDF2) or YTHDF2 overexpression (oeYTHDF2) in HOSEpiCs. Surprisingly, the mRNA levels of MAP2K4 and MAP4K4 were significantly increased in the siYTHDF2-treated cells and decreased in the oeYTHDF2-treated cells (Fig. 4A). The protein levels of MAP2K4 and MAP4K4 were consistent with the results shown in Fig. 4B. The abundance of m<sup>6</sup>A in MAP2K4 and MAP4K4 mRNAs was detected using the MeRIP-qPCR assay. We found m<sup>6</sup>A modifications in MAP2K4 and MAP4K4 mRNAs (Fig. 4C). Furthermore, RIP-qPCR analysis revealed that YTHDF2 interacted with MAP2K4 and MAP4K4 mRNAs (Fig. 4D). The stability of MAP2K4 and MAP4K4 mRNA transcripts was enhanced by a deficiency in YTHDF2 (Fig. 4E). To further confirm whether oeYTHDF2 has an impact on MAP2K4 and MAP4K4 mRNA stability, we conducted another mRNA stability assay. The data suggest that oeYTHDF2 increased the instability of MAP2K4 and MAP4K4 mRNAs (Fig. 4F). Furthermore, the results of the poly(A) tail (PAT) assay showed that YTHDF2 suppression caused an increase in poly(A) tail lengths and that YTHDF2 overexpression shortened the poly(A) tail of the MAP2K4 and

**Figure 4** Melatonin regulates the stability of MAP2K4 and MAP4K4 mRNAs in a YTHDF2-dependent manner. (A) The expression levels of MAP2K4 and MAP4K4 in HOSEpiCs that were transfected with negative control siRNA (NC), siYTHDF2 or empty vector (Ctr), and oeYTHDF2 and subjected to retrovirus-mediated expression of H-RasV12 for 8 days were measured using RT-PCR. (B) The protein levels of MAP2K4 and MAP4K4 levels were measured using Western blotting. (C) MeRIP-qPCR analysis of m<sup>6</sup>A abundance in MAP2K4 and MAP4K4 mRNAs. (D) MAP2K4 and MAP4K4 gene-specific YTHDF2 RIP-qPCR assays in HOSEpiCs. The value obtained for the IgG was set to 1. Error bars indicate the mean  $\pm$  standard error of the mean,  $n = 3$ . (E,F) HOSEpiCs that were transfected with negative control siRNA (NC), siYTHDF2 or empty vector (Ctr), and oeYTHDF2 were subjected to retrovirus-mediated expression of H-RasV12 for 8 days; then, 5  $\mu$ g/mL actinomycin D was added to inhibit global mRNA transcription for 0 h, 2 h, and 4 h. MAP2K4 and MAP4K4 expression levels were measured using qRT-PCR.  $\beta$ -actin was used as a normalization reference. (G,H) Results of the PAT assay showing poly(A) tail lengths of the indicated transcripts with different MAP2K4 and MAP4K4 3'-UTRs. The results are shown as the mean  $\pm$  standard deviation of three independent experiments.  $P < 0.05$  and  $P < 0.01$  were considered statistically significant using two-sided Student's  $t$ -test. \*,  $P < 0.05$ ; \*\*,  $P < 0.01$ .



MAP4K4 3'-UTR transcripts (Fig. 4G, H). Altogether, these results showed that melatonin might play a crucial role in increasing the instability of MAP2K4 and MAP4K4 mRNAs by upregulating the expression of YTHDF2.

### Melatonin modulates MAPK-NF- $\kappa$ B pathway activation

Given that the components of the MAPK and NF- $\kappa$ B pathways can be phosphorylated by upstream phosphatases, we sought to explore the relationship between melatonin and the activation of MAPK and NF- $\kappa$ B. We successfully knocked down MAPK in HOSEpiCs using specific siRNAs (Fig. 5A). Melatonin inhibited the NF- $\kappa$ B pathway activation during senescence; this inhibition was reversed by a deficiency in MAPK (Fig. 5B). Consistent with the Western blotting results, MAPK deficiency played a positive role in the activation of NF- $\kappa$ B pathway as determined using immunofluorescence analysis (Fig. 5C).

### Melatonin regulates the extent of NF- $\kappa$ B-binding to SASP genes

To demonstrate the binding of the proteins, as annotated in Fig. 6, to their target genes, we performed a chromatin immunoprecipitation (ChIP) of the promoter elements (-1 kb to +1 kb) of SASP genes in the presence or absence of H-RasV12 and with melatonin treatment.

ChIP-qPCR was used to analyze no-antibody control (NA), NF- $\kappa$ B, H3K27ac, and H3 (positive control). Remarkably, after Ras treatment without subsequent melatonin treatment, the promoter regions of the SASP genes were enriched for NF- $\kappa$ B (Fig. 6A). The control marker H3 was pulled down evenly (Fig. 6B). To highlight this novel mechanism of melatonin-oriented chromatin environment for controlling SASP expression, we have illustrated the loci of IL-6 in Fig. 6C to show that NF- $\kappa$ B is essential for the expression of SASP. NF- $\kappa$ B and H3K27ac were analogously enriched at the IL-6 promoter in cells with Ras-induced senescence; melatonin could prevent NF- $\kappa$ B and H3K27ac from binding to these loci. As illustrated, NF- $\kappa$ B (0.59% of the input in Ras-treated group vs. 0.31% of the input in Ras and melatonin-treated group,  $P < 0.05$ ) and H3K27ac (0.60% of the input in Ras-treated group vs. 0.30% of the input in Ras and melatonin-treated group,  $P < 0.05$ ) were enriched at the IL-6 promoter in HOSEpiCs with Ras-induced senescence; melatonin blocked this enrichment.

Altogether, these results indicate that melatonin has an antagonistic effect against Ras-induced senescence of HOSEpiCs by regulating the extent of NF- $\kappa$ B-binding to the SASP gene. Our findings provide insight into the mechanism by which melatonin suppresses ovarian aging.

## Discussion

Here, we discovered that the oncogene Ras could induce the senescence of human ovarian epithelial cells characterized by morphological changes, persistent DNA damage response (DDR), and the SASP. Moreover, we discovered that Ras could specifically decrease the expression of the RNA-binding protein YTHDF2 via ROS activation. YTHDF2 suppression increased the expression of MAP2K4 and MAP4K4 by stabilizing the related mRNA transcripts; this triggered the activation of NF- $\kappa$ B and SASP. Finally, excessive SASP led to the senescence of the affected cells. Importantly, the present study demonstrated that melatonin, as a classical antioxidant, could effectively decrease SASP and the senescence of human ovarian epithelial cells by inhibiting the ROS-YTHDF2-MAP2K4/MAP4K4-NF- $\kappa$ B pathway (Model, Fig. 7).

Ovarian aging, a special type of organ senescence, is characterized by a significant reduction in the number of primordial follicles and the quality of the oocytes.<sup>4,36</sup> Previous research has indicated that ovarian aging could lead to menopause, female infertility, and an increased incidence of chromosomal aberrations.<sup>22</sup> Ovarian epithelial cells that express claudin can increase the activity of matrix metalloproteinase-2 (MMP-2).<sup>37</sup> Moreover, the transformation of ovarian epithelial cells has been reported to give rise to the majority of ovarian tumors.<sup>38</sup> The therapeutic strategies for ovarian aging include androgen supplementation, short-term rapamycin treatment, and moxibustion; however, their use are still limited due to their side effects or poor efficacy.<sup>6-8</sup> Abnormal oxidative stress is considered an important pathological mechanism of ovarian aging.<sup>39</sup> The accumulation of oxidative damage in oocytes is the major contributing factor for ovarian aging.<sup>22</sup> It has been reported that melatonin was used in the treatment of ovarian aging. For example, melatonin can prevent postovulatory oocyte aging by inhibiting oxidative stress-induced cellular damage and apoptosis.<sup>40</sup> Melatonin is also effective in suppressing lipoperoxidation, which delays ovarian aging.<sup>41</sup>

m<sup>6</sup>A has been identified as the most frequent RNA modification in eukaryotes and is produced by methyltransferases (writers).<sup>42</sup> Demethylases (erasers) and effectors (readers) are also involved in its regulation.<sup>43</sup> m<sup>6</sup>A plays a crucial role in RNA metabolism, including mRNA stability, translation efficiency, and alternative splicing, which influence diverse biological processes.<sup>44,45</sup> It has been demonstrated that m<sup>6</sup>A implicates diverse human diseases and disorders, such as cancer, obesity, diabetes, and infertility.<sup>46-48</sup> Recently, m<sup>6</sup>A has been shown to cause DDR to the enzyme of obesity-associated gene (FTO) and methyltransferase-like 3 (METTL3).<sup>49</sup> Accumulating evidence also suggests that IGF2BPs, m<sup>6</sup>A readers, may

**Figure 5** Melatonin regulates the MAPK-NF- $\kappa$ B pathway activation. (A) Western blot analysis of RNA interference efficiency in HOSEpiCs transfected with scrambled or MAPK siRNAs. (B) Western blot analysis of the related proteins in NF- $\kappa$ B pathway activation in H-RasV12-induced senescent HOSEpiCs treated with or without melatonin using siRNA (siMAPK). HOSEpiCs were transfected with scramble siRNA as a control. (C) Immunofluorescence analysis of phosphorylated NF- $\kappa$ B (pNF- $\kappa$ B) in H-RasV12-induced senescent HOSEpiCs treated with or without melatonin and in the presence or absence of siMAPK. The nuclei were counterstained with DAPI (blue); scale bar, 50  $\mu$ m. The results are presented as the mean  $\pm$  standard deviation of three independent experiments. \*\*,  $P < 0.01$ ; \*\*\* $P < 0.001$ .

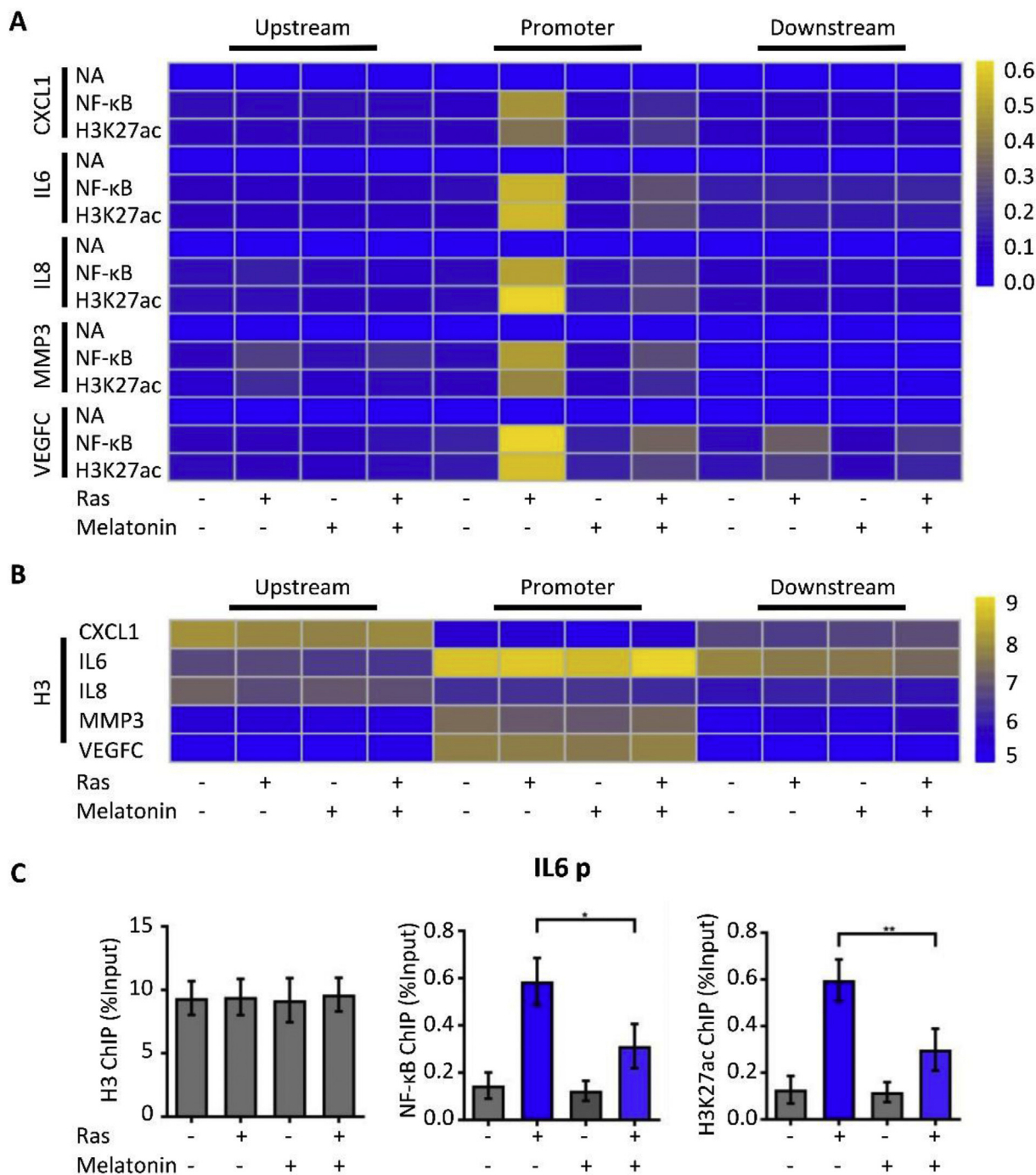


**Figure 6** Melatonin modulates the extent of NF-κB-binding to SASP genes. (A) To demonstrate the binding of the indicated proteins to their target genes, a heatmap was generated according to ChIP-qPCR values. The ChIP-qPCR enrichments of no-antibody control (NA), NF-κB, H3K27ac, and H3 using primers spanning from -1 kb to +1 kb of the indicated SASP genes are arrayed from blue (no enrichment) to yellow (maximal enrichment). (B) The control H3 protein co-precipitated evenly with the ChIP targets. A heatmap was generated according to the ChIP-qPCR values of histone H3, which were between -1 kb and +1 kb of the indicated genes. (C) Representative ChIP-qPCR values of the IL-6 gene selected from the experiments described in (A). Statistical values are presented as the mean ± standard error of three independent experiments. A  $P < 0.05$  was considered statistically significant using one-way analysis of variance. \*,  $P < 0.05$ .

contribute to hematopoietic stem cell and leukemia development by promoting mRNA stability and protein translation.<sup>50–53</sup> In addition, RNA m<sup>6</sup>A modification has been reported to be closely related to gene expression,

particularly in inflammatory cytokines. Liu et al demonstrated that the reduction of m<sup>6</sup>A modification that is induced by CC-chemokine receptor 7 upregulated lnc-Dpf3 expression and inhibited dendritic cell migration, which

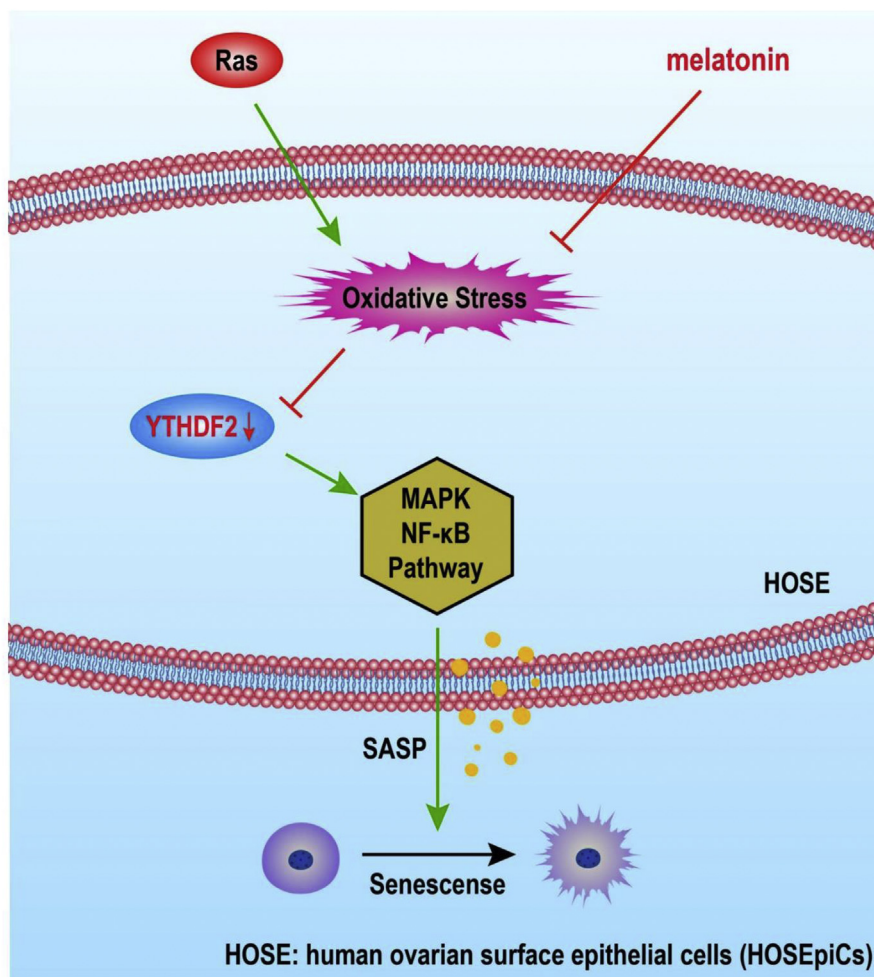


**Figure 7** Melatonin exhibited an antagonistic effect against ovarian aging via the YTHDF2-MAPK-NF- $\kappa$ B pathway. The oncogene Ras stimulates the generation of ROS to decrease the expression of YTHDF2. And then the expression of MAP2K4 and MAP4K4 are increased by stabilizing the related mRNA transcripts, which triggers the activation of NF- $\kappa$ B and SASP. Melatonin, as a classical antioxidant, effectively decreases SASP and the senescence of HOSEpiCs by inhibiting the ROS-YTHDF2-MAP2K4/MAP4K4-NF- $\kappa$ B pathway.

prevented exaggerated inflammatory responses.<sup>54</sup> Moreover, as readers of the mature mRNA m<sup>6</sup>A, YTHDF2 has been shown to attenuate LPS-induced inflammatory responses in macrophages.<sup>15</sup> SASP, which is the abnormal secretion of chemokines and cytokines related to inflammation, serves as an important signal of senescent cells.<sup>12</sup> Our study found that YTHDF2 suppression influenced the expression of SASP by activating the MAP2K4 and MAP4K4-dependent NF- $\kappa$ B pathways.

Many studies have shown that senescent cells are accompanied by a large amount of oxidative stress damage that results from the generation of reactive oxygen species (ROS). Oxidative stress is involved in the expression of SASP genes through a variety of pathways, including the ROS-JNK retrograde signaling pathway,<sup>55</sup> ROS-PKC $\delta$ -PKD1 pathway,<sup>56</sup> and ROS-p38-MAPK-p53/p21 pathway.<sup>57</sup> Recently, melatonin was reported to regulate PARP1 and control the SASP in human fetal lung fibroblast cells.<sup>58</sup> Moreover, melatonin has been reported to reduce SASP by activating NRF2 and

inhibiting NF- $\kappa$ B in adipose-derived mesenchymal stem cells (ADMSCs).<sup>59</sup> In a previous study of human periodontal ligament cells, the mechanism by which melatonin inhibits cell cycle regulators and SASP genes was reported.<sup>60</sup> Concurrently, the elevated expression of YTHDF2 and m<sup>6</sup>A upregulation was suggested to be closely related to ROS accumulation.<sup>61</sup> Melatonin can delay aging through its antagonistic effects against ROS and by regulating apelin 13<sup>62</sup> and PIN1 pathway<sup>60</sup> and reducing mitochondrial membrane potential.<sup>63</sup> Some investigations<sup>22</sup> reported that melatonin exhibits anti-aging potential in various organs and improves and treats numerous age-related diseases such as atherosclerosis and Alzheimer's disease. In particular, melatonin has been demonstrated to delay ovarian aging by attenuating oxidative stress and reducing early apoptosis.<sup>64</sup> However, the specific mechanism by which melatonin exhibits its effects needs to be further explored; this mechanism would allow the discovery of novel targets for the prevention and treatment of ovarian aging and

facilitate the precise treatment of other related diseases. As one of the most extensive RNA modifications in cells, RNA-m<sup>6</sup>A plays a critical role in the prevention and treatment of diseases. For instance, the HIF-2 $\alpha$  antagonist (PT2385) has been reported to suppress liver cancer by recovering the YTHDF2-programmed epigenetic mechanism.<sup>65</sup> RNA-m<sup>6</sup>A has also been confirmed to be associated with ovarian aging; however, its mechanism remains unclear. Here, we found that the inhibition of YTHDF2, which is the reader of RNA-m<sup>6</sup>A, specifically promoted the aging of ovarian surface epithelial cells. In our study, melatonin upregulated YTHDF2 by decreasing the generation of ROS, inactivated the NF- $\kappa$ B pathway to reduce the expression of SASP, and finally exhibited an antagonistic effect against the senescence of ovarian surface epithelial cells. Melatonin inactivates the NF- $\kappa$ B pathway to inhibit the inflammatory response via a variety of pathways, such as IGF-1, PI3K, and Akt.<sup>22</sup> Here, we identified a new ROS-YTHDF2-NF- $\kappa$ B pathway and suggest it as a novel drug target of melatonin for the treatment of ovarian aging.

The present study illustrated that YTHDF2 expression was decreased in senescent human ovarian epithelial cells. YTHDF2 suppression increased the stability and enhanced the expression of MAP2K4 and MAP4K4 mRNAs; this triggered the activation of NF- $\kappa$ B signaling and promoted the expression of SASP genes, including CXCL1, IL6, IL8, MMP3, and VEGFC. In summary, these results demonstrate that melatonin has an antagonistic effect against ovarian aging via the ROS-YTHDF2-MAPK-NF- $\kappa$ B pathway and thus holds promise for delaying ovarian aging. Although the signaling pathways and cellular stresses that influenced the differential distribution patterns of RNA methylation have been explored in this study, the underlying mechanisms of the effects of melatonin on m<sup>6</sup>A levels in the ovary still need further investigation. Further studies are also required to elucidate the functional mechanism of follicle quality, which underlies the association between melatonin and m<sup>6</sup>A levels. Moreover, the modifications in m<sup>6</sup>A regulatory factors involved in ovarian aging need to be explored in the future. Our work provides insight regarding whether melatonin is able to provide prophylactic and therapeutic effects for the treatment of reproductive diseases, such as ovarian aging.

## Conflict of interests

The authors declared no conflicts of interest.

## Funding

This research was supported by grants from National Natural Science Foundation of China (No. 31771334, 81970428, 81670421 and 81800385), Major Research Plan of the National Natural Science Foundation of China (No. 91649125), University Natural Science Research of Jiangsu Province (No. 18KJB310008 and 18KJB310010), Jiangsu Province Health and Family Planning Commission Scientific Research Project (No. H2017011), Jiangsu Provincial Medical Youth Talent (No. QNRC2016432), and Technology Development Foundation of Nanjing Medical University (No. 2017NJMUZD020 and 2017NJMU021).

This research was also supported by the program of special professor of Jiangsu Province, the program of special medical expert of Jiangsu Province and the program of innovation and entrepreneurship team plan of Jiangsu Province, China.

## Acknowledgements

This study was also supported by the Key Lab of Cardiovascular and Cerebrovascular Drugs of Jiangsu Province and by the Collaborative Innovation Center for Cardiovascular Disease Translational Medicine for data collection, analysis and interpretation.

## Appendix A. Supplementary data

Supplementary data to this article can be found online at <https://doi.org/10.1016/j.gendis.2020.08.005>.

## References

1. He S, Sharpless NE. Senescence in health and disease. *Cell*. 2017;169(6):1000–1011.
2. Childs BG, Gluscevic M, Baker DJ, et al. Senescent cells: an emerging target for diseases of ageing. *Nat Rev Drug Discov*. 2017;16(10):718–735.
3. Sharpless NE, Sherr CJ. Forging a signature of in vivo senescence. *Nat Rev Cancer*. 2015;15(7):397–408.
4. Tamura H, Kawamoto M, Sato S, et al. Long-term melatonin treatment delays ovarian aging. *J Pineal Res*. 2017;62(2):e12381.
5. Zhang L, Zhang Z, Wang J, et al. Melatonin regulates the activities of ovary and delays the fertility decline in female animals via MT1/AMPK pathway. *J Pineal Res*. 2019;66(3):e12550.
6. Sunkara SK, Coomarasamy A, Arlt W, Bhattacharya S. Should androgen supplementation be used for poor ovarian response in IVF? *Hum Reprod*. 2012;27(3):637–640.
7. Dou X, Sun Y, Li J, et al. Short-term rapamycin treatment increases ovarian lifespan in young and middle-aged female mice. *Aging Cell*. 2017;16(4):825–836.
8. Yang X, Wang W, Zhang Y, Wang J, Huang F. Moxibustion improves ovary function by suppressing apoptosis events and upregulating antioxidant defenses in natural aging ovary. *Life Sci*. 2019;229:166–172.
9. Acosta JC, Banito A, Wuestefeld T, et al. A complex secretory program orchestrated by the inflammasome controls paracrine senescence. *Nat Cell Biol*. 2013;15(8):978–990.
10. Papatheodoridi AM, Chrysavgis L, Koutsilieris M, Chatzigeorgiou A. The role of senescence in the development of nonalcoholic fatty liver disease and progression to nonalcoholic steatohepatitis. *Hepatology*. 2020;71(1):363–374.
11. Wiggins KA, Parry AJ, Cassidy LD, et al. IL-1 $\alpha$  cleavage by inflammatory caspases of the noncanonical inflammasome controls the senescence-associated secretory phenotype. *Aging Cell*. 2019;18(3):e12946.
12. Coppe JP, Desprez PY, Krtolica A, Campisi J. The senescence-associated secretory phenotype: the dark side of tumor suppression. *Annu Rev Pathol*. 2010;5:99–118.
13. Roundtree IA, Evans ME, Pan T, He C. Dynamic RNA modifications in gene expression regulation. *Cell*. 2017;169(7):1187–1200.
14. Meyer KD, Saletore Y, Zumbo P, Elemento O, Mason CE, Jaffrey SR. Comprehensive analysis of mRNA methylation

- reveals enrichment in 3' UTRs and near stop codons. *Cell*. 2012;149(7):1635–1646.
15. Yu R, Li Q, Feng Z, Cai L, Xu Q. m6A reader YTHDF2 regulates LPS-induced inflammatory response. *Int J Mol Sci*. 2019;20(6):1323.
  16. Nilsen TW. Molecular biology. Internal mRNA methylation finally finds functions. *Science*. 2014;343(6176):1207–1208.
  17. Rauch S, He C, Dickinson BC. Targeted m(6)A reader proteins to study epitranscriptomic regulation of single RNAs. *J Am Chem Soc*. 2018;140(38):11974–11981.
  18. Lee Y, Choe J, Park OH, Kim YK. Molecular mechanisms driving mRNA degradation by m(6)A modification. *Trends Genet*. 2020;36(3):177–188.
  19. Li Q, Li X, Tang H, et al. NSUN2-mediated m5C methylation and METTL3/METTL14-mediated m6A methylation cooperatively enhance p21 translation. *J Cell Biochem*. 2017;118(9):2587–2598.
  20. Huang B, Ding C, Zou Q, Wang W, Li H. Cyclophosphamide regulates N6-methyladenosine and m6A RNA enzyme levels in human granulosa cells and in ovaries of a premature ovarian aging mouse model. *Front Endocrinol (Lausanne)*. 2019;10:415.
  21. Jahanban-Esfahlan R, Mehrzadi S, Reiter RJ, et al. Melatonin in regulation of inflammatory pathways in rheumatoid arthritis and osteoarthritis: involvement of circadian clock genes. *Br J Pharmacol*. 2018;175(16):3230–3238.
  22. Majidinia M, Reiter RJ, Shakouri SK, Yousefi B. The role of melatonin, a multitasking molecule, in retarding the processes of ageing. *Ageing Res Rev*. 2018;47:198–213.
  23. Suofu Y, Li W, Jean-Alphonse FG, et al. Dual role of mitochondria in producing melatonin and driving GPCR signaling to block cytochrome c release. *Proc Natl Acad Sci U S A*. 2017;114(38):E7997–E8006.
  24. He C, Wang J, Zhang Z, et al. Mitochondria synthesize melatonin to ameliorate its function and improve mice oocyte's quality under in vitro conditions. *Int J Mol Sci*. 2016;17(6):939.
  25. Bizzarri M, Proietti S, Cucina A, Reiter RJ. Molecular mechanisms of the pro-apoptotic actions of melatonin in cancer: a review. *Expert Opin Ther Targets*. 2013;17(12):1483–1496.
  26. Rong B, Feng R, Liu C, Wu Q, Sun C. Reduced delivery of epididymal adipocyte-derived exosomal resistin is essential for melatonin ameliorating hepatic steatosis in mice. *J Pineal Res*. 2019;66(4):e12561.
  27. Nicke B, Bastien J, Khanna SJ, et al. Involvement of MINK, a Ste20 family kinase, in Ras oncogene-induced growth arrest in human ovarian surface epithelial cells. *Mol Cell*. 2005;20(5):673–685.
  28. Chen H, Ruiz PD, McKimpton WM, Novikov L, Kitsis RN, Gamble MJ. MacroH2A1 and ATM play opposing roles in paracrine senescence and the senescence-associated secretory phenotype. *Mol Cell*. 2015;59(5):719–731.
  29. Samsonraj RM, Raghunath M, Hui JH, Ling L, Nurcombe V, Cool SM. Telomere length analysis of human mesenchymal stem cells by quantitative PCR. *Gene*. 2013;519(2):348–355.
  30. Lin X, Chai G, Wu Y, et al. RNA m(6)A methylation regulates the epithelial mesenchymal transition of cancer cells and translation of Snail. *Nat Commun*. 2019;10(1):2065.
  31. Salles FJ, Strickland S. Analysis of poly(A) tail lengths by PCR: the PAT assay. *Methods Mol Biol*. 1999;118:441–448.
  32. Lichinchi G, Gao S, Saletore Y, et al. Dynamics of the human and viral m(6)A RNA methylomes during HIV-1 infection of T cells. *Nat Microbiol*. 2016;1:16011.
  33. Chen H, Ruiz PD, Novikov L, Casill AD, Park JW, Gamble MJ. MacroH2A1.1 and PARP-1 cooperate to regulate transcription by promoting CBP-mediated H2B acetylation. *Nat Struct Mol Biol*. 2014;21(11):981–989.
  34. Herranz N, Gallage S, Mellone M, et al. mTOR regulates MAPKAPK2 translation to control the senescence-associated secretory phenotype. *Nat Cell Biol*. 2015;17(9):1205–1217.
  35. Oubaha M, Miloudi K, Dejda A, et al. Senescence-associated secretory phenotype contributes to pathological angiogenesis in retinopathy. *Sci Transl Med*. 2016;8(362):362ra144.
  36. Zhang J, Chen Q, Du D, et al. Can ovarian aging be delayed by pharmacological strategies? *Ageing (Albany NY)*. 2019;11(2):817–832.
  37. Agarwal R, D'Souza T, Morin PJ. Claudin-3 and claudin-4 expression in ovarian epithelial cells enhances invasion and is associated with increased matrix metalloproteinase-2 activity. *Cancer Res*. 2005;65(16):7378–7385.
  38. Ismail RS, Baldwin RL, Fang J, et al. Differential gene expression between normal and tumor-derived ovarian epithelial cells. *Cancer Res*. 2000;60(23):6744–6749.
  39. Liu X, Lin X, Zhang S, et al. Lycopene ameliorates oxidative stress in the aging chicken ovary via activation of Nrf2/HO-1 pathway. *Ageing (Albany NY)*. 2018;10(8):2016–2036.
  40. Lord T, Nixon B, Jones KT, Aitken RJ. Melatonin prevents postovulatory oocyte aging in the mouse and extends the window for optimal fertilization in vitro. *Biol Reprod*. 2013;88(3):67.
  41. Chuffa LG, Amorim JP, Teixeira GR, et al. Long-term melatonin treatment reduces ovarian mass and enhances tissue antioxidant defenses during ovulation in the rat. *Braz J Med Biol Res*. 2011;44(3):217–223.
  42. Desrosiers R, Friderici K, Rottman F. Identification of methylated nucleosides in messenger RNA from Novikoff hepatoma cells. *Proc Natl Acad Sci U S A*. 1974;71(10):3971–3975.
  43. Chen J, Wang C, Fei W, Fang X, Hu X. Epitranscriptomic m6A modification in the stem cell field and its effects on cell death and survival. *Am J Cancer Res*. 2019;9(4):752–764.
  44. Wang S, Chai P, Jia R, Jia R. Novel insights on m(6)A RNA methylation in tumorigenesis: a double-edged sword. *Mol Cancer*. 2018;17(1):101.
  45. Fu Y, Dominissini D, Rechavi G, He C. Gene expression regulation mediated through reversible m(6)A RNA methylation. *Nat Rev Genet*. 2014;15(5):293–306.
  46. Shen F, Huang W, Huang JT, et al. Decreased N(6)-methyladenosine in peripheral blood RNA from diabetic patients is associated with FTO expression rather than ALKBH5. *J Clin Endocrinol Metab*. 2015;100(1):E148–E154.
  47. Daoud H, Zhang D, McMurray F, et al. Identification of a pathogenic FTO mutation by next-generation sequencing in a newborn with growth retardation and developmental delay. *J Med Genet*. 2016;53(3):200–207.
  48. Yang Y, Huang W, Huang JT, et al. Increased N6-methyladenosine in human sperm RNA as a risk factor for asthenozoospermia. *Sci Rep*. 2016;6:24345.
  49. Xiang Y, Laurent B, Hsu CH, et al. RNA m(6)A methylation regulates the ultraviolet-induced DNA damage response. *Nature*. 2017;543(7646):573–576.
  50. Li Z, Weng H, Su R, et al. FTO plays an oncogenic role in acute myeloid leukemia as a N(6)-methyladenosine RNA demethylase. *Cancer Cell*. 2017;31(1):127–141.
  51. Barbieri I, Tzelepis K, Pandolfini L, et al. Promoter-bound METTL3 maintains myeloid leukaemia by m(6)A-dependent translation control. *Nature*. 2017;552(7683):126–131.
  52. Vu LP, Pickering BF, Cheng Y, et al. The N(6)-methyladenosine (m(6)A)-forming enzyme METTL3 controls myeloid differentiation of normal hematopoietic and leukemia cells. *Nat Med*. 2017;23(11):1369–1376.
  53. Weng H, Huang H, Wu H, et al. METTL14 inhibits hematopoietic stem/progenitor differentiation and promotes leukemogenesis via mRNA m(6)A modification. *Cell Stem Cell*. 2018;22(2):191–205.
  54. Liu J, Zhang X, Chen K, et al. CCR7 chemokine receptor-inducible Inc-Dpf3 restrains dendritic cell migration by inhibiting HIF-1 $\alpha$ -mediated glycolysis. *Immunity*. 2019;50(3):600–615.

55. Vizioli MG, Liu T, Miller KN, et al. Mitochondria-to-nucleus retrograde signaling drives formation of cytoplasmic chromatin and inflammation in senescence. *Genes Dev.* 2020;34(5-6):428–445.
56. Wang P, Han L, Shen H, et al. Protein kinase D1 is essential for Ras-induced senescence and tumor suppression by regulating senescence-associated inflammation. *Proc Natl Acad Sci U S A.* 2014;111(21):7683–7688.
57. Jin HJ, Lee HJ, Heo J, et al. Senescence-associated MCP-1 secretion is dependent on a decline in BMI1 in human mesenchymal stromal cells. *Antioxid Redox Signal.* 2016;24(9):471–485.
58. Yu S, Wang X, Geng P, et al. Melatonin regulates PARP1 to control the senescence-associated secretory phenotype (SASP) in human fetal lung fibroblast cells. *J Pineal Res.* 2017;63(1):e12405.
59. Fang J, Yan Y, Teng X, et al. Melatonin prevents senescence of canine adipose-derived mesenchymal stem cells through activating NRF2 and inhibiting ER stress. *Aging (Albany NY).* 2018;10(10):2954–2972.
60. Bae WJ, Park JS, Kang SK, Kwon IK, Kim EC. Effects of melatonin and its underlying mechanism on ethanol-stimulated senescence and osteoclastic differentiation in human periodontal ligament cells and cementoblasts. *Int J Mol Sci.* 2018;19(6):1742.
61. Zhong X, Yu J, Frazier K, et al. Circadian clock regulation of hepatic lipid metabolism by modulation of m(6)A mRNA methylation. *Cell Rep.* 2018;25(7):1816–1828.
62. Zhang L, Li F, Su X, et al. Melatonin prevents lung injury by regulating apelin 13 to improve mitochondrial dysfunction. *Exp Mol Med.* 2019;51(7):1–12.
63. Song N, Kim AJ, Kim HJ, et al. Melatonin suppresses doxorubicin-induced premature senescence of A549 lung cancer cells by ameliorating mitochondrial dysfunction. *J Pineal Res.* 2012;53(4):335–343.
64. Wang T, Gao YY, Chen L, et al. Melatonin prevents post-ovulatory oocyte aging and promotes subsequent embryonic development in the pig. *Aging (Albany NY).* 2017;9(6):1552–1564.
65. Hou J, Zhang H, Liu J, et al. YTHDF2 reduction fuels inflammation and vascular abnormalization in hepatocellular carcinoma. *Mol Cancer.* 2019;18(1):163.